

A Practical System for High-Throughput Screening of Mutants of *Bacillus fastidiosus* Uricase

Tao Feng¹ · Xiaolan Yang¹ · Deqiang Wang¹ ·
Xiaolei Hu¹ · Juan Liao² · Jun Pu¹ · Xinyun Zhao³ ·
Chang-Guo Zhan³ · Fei Liao¹ 

Received: 28 May 2016 / Accepted: 5 September 2016 /
Published online: 10 September 2016
© Springer Science+Business Media New York 2016

Abstract For high-throughput screening (HTS) of *Bacillus fastidiosus* uricase mutants, a practical system was proposed. By error-prone PCR with final 1.5 mM MnCl₂, two focused libraries of mutants for A1-V158 and V150-D212 were generated separately. After induced expression of individual clones in 48-well microplates, *Escherichia coli* cells (BL21) were lysed by 1.0 M Tris-HCl at pH 9.0 in 96-well microplates at 25 °C for 7.5 ~ 10.5 h; uricase reaction was continuously monitored with 0.15 mM uric acid in 96-well plates by absorbance at 298 nm to estimate V_m/K_m by kinetic analysis of reaction curve for comparison. V_m/K_m was resistant to initial uric acid levels with an upper limit 3-fold over that of initial rates. By receiver-operator-characteristic analysis of the recognition of the one of higher activity in uricase pair whose specific activity ratio was 1.8 or 3.3, the area-under-the-curve was comparable to that with cell lysates prepared by sonication treatment. A cutoff for the maximum Youden index was thus developed to recognize positive mutants of 1-fold higher activity. Indeed, mutant L171I/Y182F/Y187F/A193S of higher activity but lower thermostability at pH 7.4 and mutant V144A of higher activity and consistent thermostability were discovered. Therefore, the proposed system was practical for HTS of uricase mutants.

Tao Feng and Xiaolan Yang contributed equally to this work.

Electronic supplementary material The online version of this article (doi:10.1007/s12010-016-2240-3) contains supplementary material, which is available to authorized users.

✉ Fei Liao
liaofeish@yeah.net; liaofeish@cqmu.edu.cn

¹ Unit for Analytical Probes and Protein Biotechnology, Key Laboratory of Medical Laboratory Diagnostics of the Education Ministry, College of Laboratory Medicine, Chongqing Medical University, No.1, Yixueyuan Road, Chongqing 400016, People's Republic of China

² Central Laboratory, Yongchuan Hospital, Chongqing Medical University, No.439, Xuanhua Road, Yongchuan, Chongqing 402160, China

³ Molecular Modeling and Biopharmaceutical Center and Department of Pharmaceutical Sciences, College of Pharmacy, University of Kentucky, 789 South Limestone Street, Lexington, KY 40536, USA

Keywords *Bacillus fastidiosus* uricase · Directed evolution · High-throughput screening · Cell lysate · Error-prone PCR

Introduction

Refractory gout as a chronic disease is a medical challenge since conventional chemical agents are ineffective or intolerable. Currently, uricase is the sole therapeutic agent to refractory gout [1–3], but repeated administration of any formulated uricases ultimately elicits immunoresponse in most patients [4, 5]. To overcome this problem, an engineered uricase of both higher activity and stronger thermostability is needed for a much smaller therapeutic dose [3]. Uricase is also an analytical tool for serum uric acid assay and preferred to have activity and thermostability as high as possible [6–9]. To enhance uricase activity and thermostability, rational design of mutants is highly efficient but technically challenging [10], while directed evolution is easily practiced providing suitable methods for high-throughput (HTP) screening of mutants [11–13]. Methods for HTP screening of mutants of higher activity are different from those for the screening of mutants of stronger thermostability. Therefore, practical methods for HTP screening of uricase mutants of higher activity are sought.

To improve enzyme activity by directed evolution, common screening methods tolerate heavy cost and low efficiency [14–20]. To save cost and time on screening of mutants, both the reduction of volumes of mutant libraries and a practical screening system are needed [16]. To reduce the volumes of mutant libraries of an enzyme, iterative saturation mutagenesis of all residues involved in catalysis is absorbing [21–23], but impractical with common uricases because their catalytic residues have not been elucidated. Fortunately, peptide fragments involved in catalysis can be rapidly identified and their random mutagenesis can give focused libraries of smaller volume. To mitigate the cost and time on the screening of mutant libraries, HTP operations with individual clones of mutants are mandatory. Up to date, the induced expression of individual mutants and lysis of their cells can be readily realized in HTP mode [24, 25], but HTP assay of uricase activity remains a great challenge.

Putatively, uricase activity can be measured as initial rate in HTP mode by quantifying uric acid (substrate) or hydrogen peroxide (product). However, no assays of hydrogen peroxide are practical for HTP assay of uricase initial rate due to the interference of residual uric acid and/or low efficiency [26–28]. On the other hand, microplate readers equipped with monochromators can determine uric acid absorbance at about 293 nm at much lower cost but higher efficiency and may work for HTP assay of uricase activity as initial rate. Inevitably, initial levels of uric acid and thus the upper limit of quantification (UOQ) of initial rate are restricted by measurable ranges of total absorbance with microplate readers and absorbance of cell lysates. Long lagging time and large intervals for recording UV absorbance of uric acid with microplate reader also reduce UOQ. There are usually large variations of initial rates derived from the decreases of substrate absorbance. Therefore, the assay of initial rate based on UV absorbance of uric acid is unfavorable for HTP screening of uricase mutants.

Uricase usually follows Michaelis-Menten kinetics characterized by Michaelis-Menten constant (K_m) and the maximal reaction rate (V_m). To recognize uricase mutants of higher activity, V_m/K_m can be estimated for comparison. In practice, V_m/K_m can be estimated by kinetic analysis of reaction process; such an approach to V_m/K_m prefers higher K_m and lower initial levels of uric acid and is resistant to the limited variations of initial uric acid levels and background absorbance [29–31]. Consequently, by continuously recording UV absorbance of uric acid in HTP mode, kinetic analysis of reaction curve may work for HTP screening of uricase mutants at lower cost and favorable efficiency. A uricase from *Bacillus fastidiosus* has

high K_m and excellent thermostability [6, 25]; it is a suitable tool for serum uric acid assay [6, 30, 32], and a promising candidate of biodrug to treat refractory gout when its activity is improved greatly [33–35]. Herein, the estimation of V_m/K_m in HTP mode was proposed for the screening of uricase mutants and tested with two small libraries of this bacterial uricase generated by error-prone PCR (epPCR); through all operations in HTP mode, two mutants of higher activity were indeed easily discovered from those two small libraries.

Material and Methods

Bacterial Strains, Plasmids, and Reagents

The expression vector pET28a harboring coding sequence of the uricase from *B. fastidiosus* as the starting material and its mutants obtained through site-directed mutagenesis were those we used previously [25]. All the enzymes (DNA polymerase, restriction enzymes, and so on) and *Escherichia coli* DH5 cells were purchased from TAKARA (Dalian, China). Competent cells of *E. coli* BL21 (DE3) was from Beijing Dingguo Changsheng Biotechnology Co. Ltd. (<http://www.dingguo.com/>). In-Fusion PCR cloning kit was purchased from Takara Clontech (<http://www.clontech.com/>). Uric acid was purchased from Sigma-Aldrich. Sodium borate, tri-(hydroxymethyl)-aminomethane (Tris) and other chemicals were domestic analytical reagents and used directly without treatment.

Mutant Library Construction

Two focused libraries of the *N*-terminus residues were generated separately, one for A1-V158 and the other for V150-D212 (the numbering of residues followed those in 4R8X.pdb [25]). Random mutagenesis was introduced by epPCR, and mutation rates were controlled by adjusting $MnCl_2$ concentrations. The transformed *E. coli* DH5 α cells of the wild-type uricase after amplification overnight at 37 °C was used for the extraction of the expression plasmid with TIANprep Mini Plasmid Kit and purification with TIANgel Mini Purification Kit (Tiangen Biotech, Beijing, China). The whole pET-28a plasmid was utilized as the template for epPCR with a pair of precise primers (Taihe Biotechnology Co. Ltd., Beijing, China). Particularly, primers were designed so that they generated PCR products containing sticky ends suitable for ligation to the pET-28a vector following the protocol of infusion cloning developed by Takara Clontech. In detail, to generate mutant libraries for the V150-D212 fragment, the forward primer was 5'-AGCACGTACTGCTAGCGGAACAGA-3' (A151-T157; the first base for V150 and the last two bases for E158) and the reverse primer was 5'-GTCT TGGTTTTCATATGCCCAACC-3' (exactly for G205-D212; the underlined bases were the recognition sites of restriction enzymes). For the A1-V150 fragment, details of primers were provided in Supplementary Table S1. For each epPCR, the reaction mixture in 100 μ L contained 7.0 mM $MgCl_2$, 0.2 mM dATP and dGTP, 1.0 mM dCTP and dTTP, 0.5 μ M of each primer, 0.1 ng of the template plasmid, and 5.0 U Taq polymerase in a buffer of 10 mM Tris-HCl at pH 8.3, 50 mM KCl, 1.5 mM $MgCl_2$. Unless stated otherwise, 0.5 mM $MnCl_2$ was employed for a low mutation rate while 1.5 mM $MnCl_2$ was used for a high mutation rate. After pretreatment at 95 °C for 5 min, the thermal cycling was 95 °C for 30 s, 60 °C for 40 s, 72 °C for 1.0 min in the order for a total of 35 cycles and terminated by the treatment at 72 °C for 7.0 min. Finally, 2.0 mM EDTA was added to the crude PCR product to alleviate the effects of Mn^{2+} on ligation, and PCR products were purified by using TIANgel Mini Purification Kit.

The expression vector was linearized by digestion at 37 °C overnight, with NheI/NdeI for the fragment V150-D212 while XbaI and NheI for the fragment A1-D150 (Supplementary Table S1), and was then recovered by gel electrophoresis with 1 % agarose. The process for the ligation of PCR products with the linearized expression vector followed the recommended protocol of the In-Fusion cloning kit. The ligated expression vectors were transformed into *E. coli* BL21 (DE3) cells for screening on agar plates, by eyesight-checking for individual transformed clones after growth for 20 h at 37 °C.

Amplification of Individual Clones, Induced Expression, and Cell Lysis in HTP Mode

Individual transformed clones from the screening plates were picked one by one for inoculation in 600 μ L TB medium plus 0.1 g/L kanamycin with 48-well plates. The cultivation mixture was shaken at 180 rpm and 37 °C for 12 h and then 100 μ L suspension of cells was withdrawn for reservation; to the residual suspension, 100 μ L IPTG solution was added for the final 0.24 g/L to induce the expression of the mutant for 18 h at 16 °C. For the reference lysis method, cells in 0.40 mL suspension from each well were harvested by centrifugation at $1180\times g$ for 5.0 min (SIGMA Laborzentrifugen 1–14, Germany) in 1.5 mL Ependorf tube, then washed, re-suspended in 1.0 mL 0.1 M Tris-HCl at pH 8.0 for sonication treatment in ice-water bath at 30 % amplitude for 2.0 min at 5-s intervals (SONICS Uibra Cell, Sonics & Materials, INC., 53 Church Hill Rd., Newtown, CT, USA); the supernatant after centrifugation at $10,625\times g$ for 5.0 min served as a sample. For HTP lysis, cell suspension in the 48-well plate was shaken rapidly for 5.0 min on Qilinbeier QB-9001 agitator and then 20 μ L suspension of cells from each well was mixed in a well of 96-well microplate with 180 μ L of the lysis buffer (1.0 M Tris-HCl at pH 9.0, containing final 1.0 mM *p*-aminobenzamidine and 0.1 % tween-20); the ratio of cell suspension to the lysis buffer in 96-well microplates was optimized after trial analysis. The mixtures of cells and the lysis buffer in 96-well microplates were agitated continuously and rapidly at $(25 \pm 2$ °C) for an indicated time to yield cell lysates that directly served as the samples prepared by HTP lysis.

HTP Assay of Uricase Activity

Uricase activity was measured with 96-well plates and BioTek EON microplate reader under the control of Gene 5.0 software. Each reaction mixture in a total of 200 μ L in a well contained 20 μ L properly diluted cell lysate and 180 μ L of 167 μ M uric acid in 0.2 M sodium borate (50 mM $\text{Na}_2\text{B}_4\text{O}_7 \cdot 10 \text{H}_2\text{O}$) at pH 9.2 [26, 31]. The solution of uric acid was pre-incubated at $(27.5 \pm 0.5$ °C) for 20 min before use and prepared every 4.0 h. Uricase reaction was initiated by the addition of uric acid solution followed by shaking of the microplate for 3.0 min. Uricase reaction curve was continuously monitored by UV absorbance at a selected wavelength that was optimized for the initial absorbance below 1.600. The molar absorption coefficient of uric acid was determined at selected wavelengths with 200 μ L solution and 96-well microplates. Absorbance data were output into MS Excel and read into computer memory for estimating uricase activity as V_m/K_m , with K_m fixed at 0.30 mM and molar absorption coefficient fixed at that determined by experimentation [29–31].

Cutoff for the Recognition of a Positive Mutant

The wild-type uricase had a specific activity of about 1.8-fold of that of the mutant L322D-SN-6His and 3.3-fold of the mutant E2R/L322D-SN-6His as described previously [25]. For

convenience, L322D-SN-6His and E2R/L322D-SN-6His served as the artificial starting enzymes while the wild-type uricase was tested as a positive mutant to test the effects of cutoffs on the recognition of positive mutants. Receiver-operator- characteristic (ROC) analysis was performed to check the decision/recognition performance. A practical cutoff for recognizing positive mutants was determined based on the maximum of Youden index.

Characterization of Uricase Mutant

Site-directed mutagenesis was performed by Taihe Biotechnology Co. Ltd. (Beijing, China). The initial rate of uricase/mutant was measured at final 75 μM uric acid at pH 9.2 in 0.20 M sodium borate buffer at 25 °C with a spectrophotometer [24]; the millimolar absorptivity of uric acid at 293 nm was preset at 11.5 $\text{mM}^{-1} \text{cm}^{-1}$ [26, 30]. One unit of uricase oxidized 1 μ mole of uric acid per min. The total proteins were quantified by the Bradford method with bovine serum albumin as the reference protein [36]. The homotetramer structure and activities of resolved components of uricase/mutants after purification by chromatography twice through DEAE-cellulose were analyzed by both non-denaturing polyacrylamide-gel-electrophoresis (PAGE) and sodium dodecylsulfate-PAGE (SDS-PAGE) [37]. Oligomer activities were examined through peroxidase-coupled staining reaction [37]. In detail, the staining solution contained uric acid saturated in 0.20 M sodium borate-boric acid at pH 8.0, plus 10 % volume of a concentrated solution of horseradish peroxidase (>200 kU/L) and its chromogenic substrate 4,4'-dimethylaminobenzidine; the gel after PAGE was quickly immersed in the staining solution in a sealed plastic bag and shaken mildly in dark [37]. Thermostability of uricase was checked for the period to reserve 50 % of initial activity in the presence of antibacterial agents in 0.20 M borate-boric acid as reported previously [25].

Other Methods

Initial rate was estimated from no less than four data bearing total absorbance changes over 0.030 by regression analysis with determination coefficient (R^2) over 0.95 [31]. As for uricase activity, the lower limit of quantification (LOQ) was the smallest one that was larger than 3-fold of the standard error of estimate for linear response (SEE) and had coefficient of variation (CV) <20 % and a deviation from the predicted value below 2-fold of SEE; UOQ was the largest one that had CV <10 % and a deviation from the predicted value below 2-fold of SEE [31]. To enhance the reliability of the LOQ and UOQ of V_m/K_m , at least seven data bearing total absorbance changes over 0.090 and the maximum substrate consumption percentage over 50 % were utilized for analysis. Experimental results were given as mean \pm standard deviation (SD) to derive coefficient of variation (CV). Statistical analysis used SPSS 19.0 for ROC analysis and MS Excel 6.0 for others. The mutation rate was estimated as the percentage of total mutations among the total number of nucleotides sequenced with the selected individual clones. The primers for molecular cloning were designed with Primer 5.0. Multiple sequence alignment was performed with DNAMAN 6.0.

Results

Estimation of V_m/K_m in HTP Mode

For reasonable operation precision, 20 μL cell lysate was transferred for activity assay. The following optimizations of the screening system employed Biotek EON microplate reader and

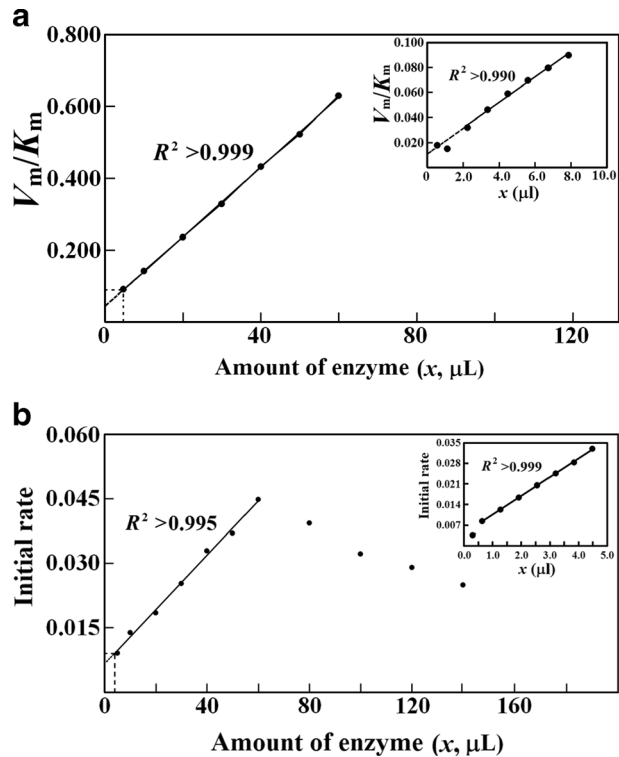
96-well microplates, with 180 μL substrate solution and 20 μL cell lysate prepared under HTP mode with 1:9 ratio of cell suspension to the alkaline lysis buffer. In this case, uric acid had the absorptivity of about $8.0 \text{ cm}^{-1}\cdot\text{mM}^{-1}$ at 293 nm, about $6.9 \text{ cm}^{-1}\cdot\text{mM}^{-1}$ at 298 nm, and about $4.9 \text{ cm}^{-1}\cdot\text{mM}^{-1}$ at 302 nm (Supplementary Fig. S1). The absorbance of uric acid decreased more rapidly than cell lysates from 293 to 302 nm. Uric acid at the first datum for analysis should thus be over 20 μM to provide the maximum net change of absorbance over 0.090 at a wavelength from 293 to 302 nm. For HTP operation, the addition of substrate solution into 96 wells of each microplate needed about 1.5 min; there should be about 3.0 min to agitate microplates for making homogenous solutions in wells. The highest absorbance should be below 1.600 for smooth reaction curves (Supplementary Fig. S2); with initial uric acid at 0.15 mM in wells containing 20 μL undiluted cell lysates from individual clones, the first recorded absorbance for 99 % cell lysates from individual clones was below 1.500 at 298 nm but over 1.500 at 293 nm (Supplementary Fig. S3). Therefore, initial uric acid at 0.15 mM in wells was used to record absorbance at 298 nm for HTP recording of reaction curves.

V_m/K_m by kinetic analysis of reaction curve was resistant to variations of background absorbance and lag time or uric acid concentrations at the first datum for analysis, but initial rates were susceptible to most of such variations (Supplementary Table S2). V_m/K_m was susceptible to the preset K_m [29–31], but it is impractical to estimate K_m for the screening of mutants. Effects of K_m on V_m/K_m were then tested with substrate consumption percentages over 60 % at each selected initial uric acid level and the wild-type uricase as a model whose K_m was about 0.30 mM [25]. When uric acid at the first analyzed datum was about 0.10 mM, the use of K_m at 0.20 mM gave V_m/K_m larger by about 10 % than those consistent V_m/K_m with K_m preset at 0.30–0.45 mM. When uric acid at the first analyzed datum was below 40 μM , however, K_m preset from 0.20 to 0.45 mM gave consistent V_m/K_m . When substrate consumption percentages were smaller, V_m/K_m showed stronger susceptibility to K_m . Lower levels of uric acid at the first analyzed data and larger substrate consumption percentages at the last analyzed data were thus preferred for the estimation of V_m/K_m . Longer reaction periods gave larger substrate consumption percentages. With 20 μL cell lysate of the wild-type uricase plus 180 μL substrate solution for final 0.15 mM uric acid in wells, reaction curves recorded within 25 min already gave robust V_m/K_m . Therefore, reaction curves were recorded within 30 min, unless otherwise stated.

When all the prerequisites for reliable V_m/K_m were met, the resulted V_m/K_m showed a linear response to quantities of the wild-type uricase. Approximated from V_m/K_m of the wild-type uricase estimated under HTP mode, the ratio of UOQ to LOQ was over 15-fold (Fig. 1a). However, initial rates for linear response covered a range of about 7-fold since its UOQ needed the quantity of the wild-type uricase below 30 % of that for the UOQ of V_m/K_m while its LOQ was just slightly smaller than that of V_m/K_m (Fig. 1b). At the UOQ of initial rate, uric acid concentration at the first recorded datum was below 70 μM . From the data for the UOQ of initial rate, CVs of V_m/K_m and initial rate were below 6 % ($n = 5$). Notably, initial rates showed a biphasic response to uricase quantities (Fig. 1b).

To screen mutants, cells should be lysed in HTP mode with consistent efficacy. Tris-HCl buffer at 1.0 M and pH 9.0 plus 0.1 % tween-20 and 1.0 mM *p*-aminobenzamidine was selected as the lysis buffer after investigations with an arylsulfatase as the model [24]. The ratio of cell suspension to the lysis buffer affected both the period for steady lysis efficacy and the necessity of pre-dilution of cell lysates before HTP assay of V_m/K_m . After optimization, the ratio of cell suspension to the lysis buffer was preset at 1:9 and the period for steady cell lysis efficacy by agitation under room temperature was 7.5–10.5 h (Supplementary Fig. S4). For the

Fig. 1 Responses of activities at initial uric acid of 0.15 mM to quantities of the wild-type uricase. **a** V_m/K_m by kinetic analysis of reaction curve; **b** initial rates



wild-type uricase, V_m/K_m with 20 μL cell lysate was $(0.20 \pm 0.06)/\text{min}$ ($n = 48$), enabling the direct assay of 3-fold higher activity of a mutant without dilution of cell lysate (Fig. 1a). By the classical initial rate method, however, the dilution of cell lysates before analysis was usually required, causing more screening labor besides unreliable results.

Recognition of Positive Mutants

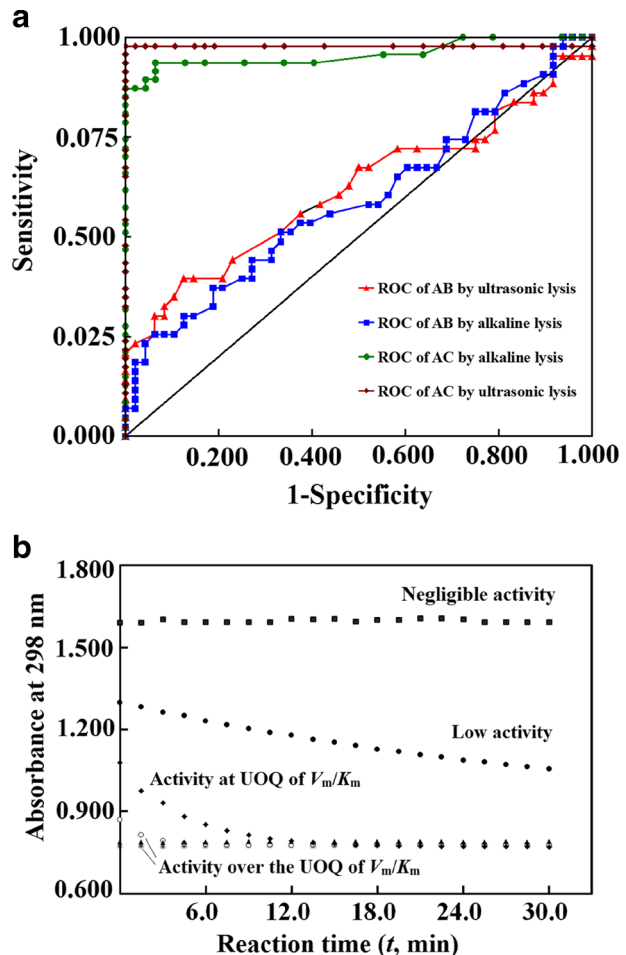
Two mutants (L322D-SN-6His and E2R/L322D-SN-6His) gave two pairs with the wild-type uricase to have the ratios of their specific activities at 1.8 and 3.3, respectively, for developing a cutoff of positive mutants through ROC analysis. Due to lower activities of those two mutants [6, 25], reaction periods were prolonged to 50 min for substrate consumption percentages over 60 % with 20 μL undiluted cell lysates as samples. CVs of V_m/K_m of those uricases (mutants) ranged from 26 to 39 % in cell lysates prepared via HTP alkaline lysis ($n = 48$), while CV ranged from 16 to 25 % in cell lysates prepared via sonication treatment ($n = 48$) (Supplementary Table S3). In fact, the induced expression of the same clone of cells in 48-well microplate, alkaline lysis of the same suspension of cells in 96-well microplate, and activity assay of the same cell lysate with 96-well microplate had CVs of 16, 6, and 3 %, respectively ($n = 48$) (Supplementary Table S4). Therefore, the variation of uricase activities in cell lysates from individual clones was primarily originated from their inherent variations of efficacy of induced expression.

To test the recognition of the wild-type uricase as a positive mutant by ROC analysis, L322D-SN-6His and E2R/L322D-SN-6His served as the artificial starting enzymes. ROC

analyses of activities in cell lysates prepared by HTP lysis gave the area-under-curve (AUC) of 0.591 for the pair with L322D-SN-6His, while AUC of 0.957 for the pair with E2R/L322D-SN-6His (Fig. 2a). Moreover, the comparison of activities in cell lysates after induced expression in 48-well microplate but lysis by sonication treatment gave AUC of 0.618 and 0.978 for those two pairs. For the maximum Youden index, the average of activities of a starting uricase in cell lysates prepared in HTP mode plus 3.6-fold SD served as the cutoff for positive mutants bearing about 1-fold higher activities (Supplementary Table S5).

Notably, a uricase mutant of extremely high activity and that of negligible activity give reaction curves bearing tiny decreases of absorbance after agitation of the microplate for 3.0 min to make homogenous solutions in wells, but can be discriminated qualitatively as follows. The absorbance at 298 nm of 20 μ L undiluted cell lysate from individual clones of the wild-type uricase plus 180 μ L borate buffer at pH 9.2 with 96-well microplates was 0.750 ± 0.085 ($n = 24$) (Fig. 2b). With 96-well microplate, the net absorbance at 298 nm of 0.15 mM uric acid in 200 μ L borate buffer at pH 9.2 was 1.050 ± 0.025 ($n = 24$), while the absorbance at 298 nm of buffer alone was 0.215 ± 0.025 ($n = 24$). As a result, the recorded

Fig 2 Recognition of a positive mutant. **a** ROC analysis of reaction curve for the recognition of the wild-type uricase (A) as a positive mutant over L322D-SN-6His (B) and E2R/L322D-SN-6His (C). Cells were amplified and induced for expression under HTP mode in 48-well microplates. For comparison, cell lysates were prepared by sonication treatment for collected cells in the same alkaline buffer lysis. For ROC analysis, AB represented the wild-type uricase and L322D-SN-6His in a pair, AC indicated the wild-type uricase and E2R/L322D-SN-6His in a pair. **b** Comparison of reaction curves to qualitatively discriminate a mutant of extremely high activity from both an inactive mutant and a mutant of low activity



initial absorbance at 298 nm of reaction mixture should be about 1.60, providing no consumption of uric acid before the recording of absorbance. In fact, after agitation of the microplate for 3.0 min to make solutions in wells, the initial absorbance at 298 nm for 20 μ L undiluted cell lysates from individual clones of the wild-type uricase and initial 0.15 mM uric acid in final 200 μ L solution varied from 1.13 to 1.46 with standard error of 0.03 ($n = 96$; Supplementary Fig. S3b). In the case of a negligible decrease of absorbance at 298 nm within the stated reaction period after agitation of 96-well microplate for 3.0 min to make solutions in wells, therefore, a mutant should have activity lower than the wild-type uricase when the initial absorbance was over 1.55, or have higher activity and serve as a candidate of positive mutants when the initial absorbance was below 1.04, at 99 % confidence limit.

Application to HTP Screening of Uricase Mutants

The components including quantities of the vector as the template and nucleotides were optimized to generate each focused library by epPCR with a pair of precise primers for the fragment A1-V158 (the epPCR product had 475 bp, Supplementary Table S1) or V150-D212 (the epPCR product had 189 bp). There were consistent yields of PCR products with $MnCl_2$ below 1.5 mM, but significant reduction of the yields of DNA fragments with $MnCl_2$ over 1.5 mM (Supplementary Fig. S5). There was an average of 8 bp mutation among 189 bp of the epPCR products with the precise primer against V150-D212 at final 1.5 mM $MnCl_2$, indicating a mutation rate of about 3.5–4.3 % (Supplementary Table S6). Differently, when the mutation rate was reduced to about 0.3 % with 0.50 mM $MnCl_2$, there were nearly 30 % active clones in a library of 400 clones for the fragment V150-D212, but ultimately no mutations were detected at all by sequencing (Supplementary Table S7).

With the pair of precise primers for the fragment A1-V158 at final 1.5 mM $MnCl_2$ in epPCR reaction mixture, a library of 800 individual clones was then generated for screening. The percentage of active clones was about 4 % while that of positive mutants was just about 0.8 % based on the cutoff of V_m/K_m for 1-fold higher activities. After sequencing, induced expression and purification by DEAE-cellulose chromatography once, only mutant V144A exhibited the apparent specific activity of about 130 % of that of the wild-type uricase. Moreover, after DEAE-cellulose chromatography and preparative PAGE [32], the highest specific activity of mutant V144A was about 13.5 kU/g and that of the wild-type uricase was about 9.5 kU/g, indicating about 50 % improvement of specific activity of the mutant. To our surprise, its thermostability at pH 7.4 or 9.2, K_m at pH 9.2 and susceptibility of activity to pH were consistent with those of the wild-type uricase [25].

To further test the application of the proposed HTP screening system, another focused small library was generated by epPCR with the pair of precise primers for the fragment V150-D212 at final 1.50 mM $MnCl_2$. After about 400 individual clones were screened in HTP mode, only about 5 % clones exhibited detectable activities, and one positive mutant was found based on the cutoff of V_m/K_m for 1-fold higher activities. The positive mutant had seven mutated bases, but four mutated amino acid residues plus three sites of silent mutation (L171I/Y182F/Y187F/A193S) (Fig. 3a; Supplementary Fig. S6). This mutant had the molecular weight of about 36 kDa (Supplementary Fig. S7). After purification twice through DEAE-cellulose with Tris-HCl buffer at pH 8.0, the specific activity at pH 9.2 reached (8.3 ± 0.3 kU/g) for the mutant ($n = 2$), while was about 6.8 ± 0.3 kU/g for the wild-type uricase ($n = 3$). The ratio of the activity of the mutant at pH 7.4 to that at pH 9.2 was (27 ± 3 %) ($n = 2$), comparable to that of

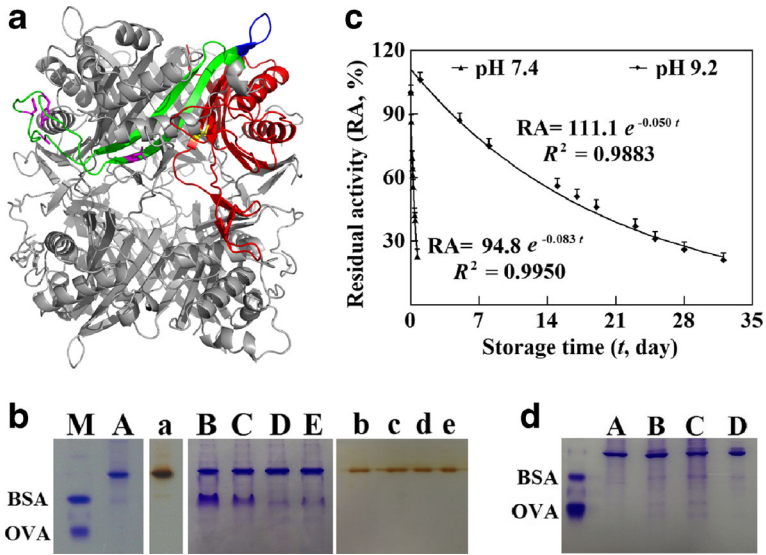


Fig 3 Characterization of the mutant L171I/Y182F/Y187F/A193S. **a** Cartoon of the wild-type uricase (PDB id 4R8X) to show the two fragments for random mutagenesis and the detected mutation in the mutants [23]. The fragment A1-E158 was presented in *red*, V150-D212 was shown in *green* while their overlapped region V150-E158 was displayed in *blue*. The four detected mutation sites in the fragment of V150-D212 were presented as sticks in *magenta*; V144A as the mutation site detected in the fragment A1-E158 was shown in *yellow*. The three silent mutation sites at I166, Y180, R196 were not shown. **b** The resolution of oligomers of the wild-type uricase and the synergistic mutant by non-denaturing PAGE, before and after induced association by its substrate uric acid and competitive inhibitors (xanthine and oxonate). Proteins were stained with coomassie brilliant R250 as *blue bands* while uricase activity was stained as *brown bands* with uric acid plus peroxidase and chromogenic substrate 4,4'-dimethylaminobenzidine (*M*: bovine serum albumin (*BSA*) and ovalbumin (*OVA*) as the markers; *A* and *a*: the wild-type uricase; *B* and *b*: the purified synergistic mutant; *C* and *c*: the synergistic mutant after induced association by uric acid; *D* and *d*: the synergistic mutant after induced association by xanthine; *E* and *e*: the synergistic mutant after induced association by oxonate. **c** Dynamic change of residual activity of the synergistic mutant during storage at pH 9.2 or 7.4 in 0.20 M sodium borate–boric acid buffer. **d** The resolution of oligomers and staining for proteins after non-denaturing PAGE of one-by-one mutation of the four sites (*M*: BSA and OVA as markers; *A*: L171I; *B*: Y182F; *C*: Y187F; *D*: A193S)

the wild-type uricase [25] (Supplementary Table S8). The mutant had K_m of about 0.27 mM at pH 9.2, consistent with that of the wild-type uricase [32]. At pH 7.4, K_m of the mutant or the wild-type uricase was too large to be estimated by any common methods. However, the mutant showed some unexpected properties.

In 20 mM Tris-HCl at pH 8.0, the wild-type bacterial uricase showed the solubility over 15 g/L at pH 8.0, but the mutant L171I/Y182F/Y187F/A193S exhibited much lower solubility (Supplementary Fig. S7). The wild-type uricase exhibited as active homotetramer, but the mutant appeared as active homotetramer plus nearly 50 % inactive homodimers. Unexpectedly, the binding of substrate or oxonate induced the association of homodimers of the mutant into homotetramer (Fig. 3b). To address the inherent specific activity, the homotetramer of the mutant was resolved by preparative PAGE [32, 37] and found to have the specific activity of 13.5 kU/g, indicating about 50 % improvement of activity. Notably, during thermostabilization at 37 °C, the half-life of the mutant activity was just about 7.0 h at pH 7.4 but about 15 days at pH 9.2 (Fig. 3c). Differently, the mutant reserved over 90 % of its activity at 4 °C after storage for 4.5 months in 0.10 M Tris-HCl at pH 8.0, comparable to that of the wild-type uricase [6, 23]. Among the four sites, one-by-one mutation always gave mutants as homotetramers

(Fig. 3d); none of the single mutation increased the activity, but Y187F or A193S caused moderate decrease of thermostability at pH 7.4 and 37 °C (Table 1; Supplementary Fig. S8).

Discussion

Microplate readers usually show random absorbance errors below 0.003 at wavelengths from 293 to 302 nm. For kinetic analysis of uricase reaction curve, an effective datum requires absorbance change from its previous or further previous one over 0.006. For reliable V_m/K_m , kinetic analysis of reaction curve prefers substrate concentration below one-third of K_m at the first analyzed datum and requires sufficient effective data bearing high precision and substrate consumption percentages over 50 % [29–31]. The net changes of absorbance over 0.090 can provide precise data considering the random absorbance error of 0.003 with microplate reader. In general, the minimal number of effective data for reliable V_m/K_m is seven [29–31]. In practice, the maximum number of effective data in a reaction curve is determined primarily by the recording intervals, reaction period, and initial substrate concentration and enzyme activity. The shortest recording intervals are about 1.0 min with 96 wells. Longer reaction periods reduce assay efficiency; a practical reaction period is about 30 min, which together with the minimal substrate consumption percentage determines the LOQ of V_m/K_m [29–31]. There is the background absorbance of cell lysates; red shift of the wavelength for monitoring reaction curves reduces the absorbance of both uric acid and cell lysates. The wild-type uricase has K_m of about 0.30 mM [25, 32], and uric acid at the first analyzed datum much below 0.10 mM is thus preferable for reliable V_m/K_m . Due to the need of a long time for agitation of microplates to make solutions, however, initial uric acid concentrations before the addition of uricase sample should be over 0.10 mM so that there can be sufficient effective data with mutants of higher activity. After optimizations, initial uric acid at 0.15 mM was used to continuously record absorbance of uric acid at 298 nm with 96-well microplate.

Under conditions after systematic optimizations, the linear response of V_m/K_m to uricase quantities gave a UOQ nearly three times that of initial rates while their LOQs showed a smaller difference; to uricase quantities, there was a monotonic response of V_m/K_m , but a biphasic response of initial rates to complicate the recognition of positive mutants based on initial rate (Fig. 1a and Fig. 1b). These results supported that the estimation of V_m/K_m by kinetic analysis of reaction curve was advantageous for HTP screening of uricase mutants. By

Table 1 Characterization of the mutant L171I/Y182F/Y187F/A193S

Uricase	Wild-type	L171I/Y182F/ Y187F/A193S	L171I	Y182F	Y187F	A193S
Specific activity (kU/g)	6.8 ± 0.3 (2)	8.3 ± 0.4 (2)	5.2 ± 0.3 (2)	4.8 ± 0.3 (2)	3.3 ± 0.2 (2)	2.0 ± 0.2 (2)
K _m (mM) at pH 9.2	0.31	0.27	0.36	0.44	0.35	0.49
Half-life at pH 7.4 and 37 °C (day)	22 ± 2	0.3 ± 0.02	20 ± 2 (2)	26 ± 3 (2)	2.6 ± 3 (2)	8.5 ± 2 (2)

Number in parenthesis was for independent preparation of samples for assays in duplicate. There were exponential decreases of activity of those mutants under physiological conditions and thus half-life time of activity during storage was estimated (Supplementary Fig. S7)

ROC analysis of V_m/K_m , uricase mutants of moderate improvement of activity were recognized against the starting ones with reasonable reliability (Fig. 2a), supporting the feasibility of the proposed system for HTP screening of uricase mutants. However, the discrimination of a mutant of extremely high activity from that of negligible activity is a challenge since it was impractical to estimate their V_m/K_m . Fortunately, after a long lag time to record reaction curve by microplate reader, the substrate may be exhausted with a mutant of extremely high activity, but will exhibit little consumption with a mutant of negligible activity. Namely, a uricase mutant of extremely high activity gave the absorbance at the first recorded datum much smaller than that with a mutant of negligible activity (Fig. 2b); such a difference aided the discrimination of most of such two types of mutants, when there was an initial uric acid level high enough so that the net absorbance of uric acid was much higher than the variation of the absorbance of cell lysates. This discrimination approach may be applicable to diverse enzymes when their activities were measured by quantifying substrate absorbance.

To test the applicability of the proposed HTP screening system, short fragments close to the active site of the bacterial uricase were utilized as the templates to construct representative focused libraries by epPCR [11–16, 38, 39]. The accessibility to restriction enzymes for the ligation of epPCR products with the linearized expression vector was another criterion for the selection of templates for epPCR. The *N*-terminus residues of *B. fastidiosus* uricase were crucial for catalysis [25]; a 63-residue peptide (V150-D212) formed a loop to isolate the active site of *B. fastidiosus* uricase from bulk solution (Fig. 3a); encoding sequences for these two peptides served as templates to generate focused libraries by epPCR. Meanwhile, considering the cost and time on screening, the yield of false positive mutants was a heavy concern; the use of higher mutation rate gave more mutants of no activity and, thus, fewer false positive mutants by a suitable screening method. In the two small focused libraries generated separately by epPCR at high mutation rates, one with A1-V158 and the other with V150-D212 as the templates, two mutants of higher activity were indeed discovered.

For the mutant L171I/Y182F/Y187F/A193S, the removal of homodimer by PAGE was expected to increase homotetramer activity by 1-fold, since the homodimer accounted for nearly 50 % of total proteins in the preparation (Fig. 3b). In fact, the improvement of the activity of the homotetramer of the mutant reached only about 50 %. The binding of substrate, xanthine and oxonate, induced the association of the homodimer of the mutant into active homotetramer (Fig. 3b); the activity of the mutant as a mixture of homodimer and homotetramer should be higher than 50 % of that of the resolved homotetramer due to the conversion of homodimers into homotetramer upon the addition of uric acid to measure its activity. Meanwhile, its lower thermostability may also account partially for moderate improvement of its activity after the removal of homodimers. There should be synergistic effects of those mutated sites to disrupt the noncovalent interaction networks and cause lower thermostability of the mutant [40]. On the other hand, for the mutant V144A, most kinetic properties besides thermostability remained consistent with those of the wild-type uricase. However, the effect of mutation on the activity of the mutant V144A was a puzzle since the mutation site had a reasonable distance from the putative active site [25]. It was a pity that both positive mutants exhibited limited improvement of activity, but the generation of larger libraries for HTP screening may give mutants of larger improvement of activity.

Up to date, few reports dealing with molecular engineering of uricases are searchable in open databases. The catalytic mechanism and sequence–activity relationship of *Bacillus subtilis* uricase were partially revealed [41]; its HTP screening system had long been reported [27]. However, none of its mutants of improved activity had been reported yet. *Arthrobacter*

globiformis uricase was recently commercialized by Asahi-kasei (product T129, maximum ~20 kU/g) and Sigma-Aldrich (product U7128, maximum 15~30 kU/g), but no details related to its molecular engineering had been reported [6, 42, 43]. The dependence of activities of common uricases on their complicated homotetramer structures besides their unknown catalytic mechanism may be the primary hindrance on rational design of uricase mutants of higher activity; the lack of a practical HTP screening system may be the principal determinant of the discovery of uricase mutants of higher activity by directed evolution. In fact, peroxidase-coupled colorimetric assay of hydrogen peroxide was once proposed for HTP screening of uricase mutants [27], but in fact inapplicable since residual uric acid at high levels caused large negative interference with peroxidase-coupled assay of hydrogen peroxide (unpublished). Xylenol-orange-assay-of-hydrogen-peroxide tolerated uric acid at limited levels, but its labor and lower efficiency still caused problems for HTP screening of uricase mutants [28]. Notably, positive mutants of moderate improvement of activity were readily discovered from two representative small libraries of the bacterial uricase, supporting the effectiveness of the proposed HTP screening system. A library of uricase can be designed by anyone suitable approach; however, the proposed HTP screening system may be the unique and practical approach to uricase mutants at favorable cost and high efficiency.

Conclusion

The proposed screening system through HTP operations for induced expression, cell lysis, and activity assay was practical for the screening of libraries of uricase mutants. In the proposed screening system, the monitor of UV absorbance of uric acid for the estimation of V_m/K_m by kinetic analysis of reaction curve provided much lower cost, higher analysis efficiency, and the strong resistance of V_m/K_m to common interferences; the higher UOQ of uricase activity as V_m/K_m and the resistance of V_m/K_m to initial levels of uric acid and background absorbance enhanced the discovery of positive mutants from libraries.

AUC, the area-under - curve; CV, coefficient of variation; epPCR, error-prone PCR; HTP, high-throughput; HTS, high-throughput screening; K_m , Michaelis-Menten constant; LOQ, the lower limit of quantification; ROC, receiver - operator - characteristic; SD, standard deviation; SEE, the standard error of estimate for linear response; UOQ, the upper limit of quantification; V_m , the maximal reaction rate.

Acknowledgments This work was supported by National Natural Science Foundation of China (nos. 30672139, 31570862 and 21402108), the Sciences and Technology Commission of Yuzhong District of Chongqing (no. 20130135), the Education Ministry of China (no. 20125503110007), and Chongqing Sciences and Technology Commission (CSTC2011BA5039). Some mutants reported here were claimed for invention patent in China (application no. 201610093491.8).

References

1. Fels, E., & Sundy, J. S. (2008). Refractory gout, what is it and what to do about it? *Current Opinion in Rheumatology*, 20, 198–202.
2. George, R. L., & Sundy, J. S. (2012). Pegloticase for treating refractory chronic gout. *Drugs Today*, 48, 441–449.
3. Yang, X., Yuan, Y., Zhan, C.-G., & Liao, F. (2012). Uricase as therapeutic agents to treat refractory gout, current states and future directions. *Drug Development Research*, 73, 66–72.

4. Sundry, J. S., Ganson, N. J., Kelly, S. J., Scarlett, E. L., Rehrig, C. D., Huang, W., & Hershfield, M. S. (2007). Pharmacokinetics and pharmacodynamics of intravenous PEGylated recombinant mammalian urate oxidase in patients with refractory gout. *Arthritis and Rheumatism*, *56*, 1021–1028.
5. Yue, C. S., Huang, W., Alton, M., Maroli, A. N., Waltrip, R. W., Wright, D., & Marco, M. D. (2008). Population pharmacokinetic and pharmacodynamic analysis of pegloticase in subjects with hyperuricemia and treatment-failure gout. *Journal of Clinical Pharmacology*, *48*, 708–718.
6. Huang, Y., Chen, Y., Yang, X., Zhao, H., Hu, X., Pu, J., Liao, J., Long, G., & Liao, F. (2015). Optimization of pH values to formulate the bireagent kit for serum uric acid assay. *Biotechnology and Applied Biochemistry*, *62*, 137–144.
7. Zhao, Y., Yang, X., Lu, W., Liao, H., & Liao, F. (2009). Uricase based method for determination of uric acid in serum. *Microchimica Acta*, *164*, 1–6.
8. Arora, K., Choudhary, M., & Malhotra, B. D. (2014). Enhancing performance of uricase using multiwalled carbon nanotube doped polyaniline. *Applied Biochemistry and Biotechnology*, *174*, 1174–1187.
9. Chauhan, N., Kumar, A., & Pundir, C. S. (2014). Construction of an uricase nanoparticles modified an electrode for amperometric determination of uric acid. *Applied Biochemistry and Biotechnology*, *174*, 1683–1694.
10. Zheng, F., & Zhan, C.-G. (2008). Rational design of an enzyme mutant for anti-cocaine therapeutics. *Journal of Computer-Aided Molecular Design*, *22*, 661–671.
11. Morre, J. C., & Arnold, F. H. (1996). Directed evolution of a *para*-nitrobenzyl esterase for aqueous-organic solvents. *Nature Biotechnology*, *14*, 458–467.
12. Aharoni, A., Griffiths, A. D., & Tawfik, D. S. (2005). High-throughput screens and selections of enzyme-encoding genes. *Current Opinion in Chemical Biology*, *9*, 210–216.
13. Sen, S., Venkata Dasu, V., & Mandal, B. (2007). Developments in directed evolution for improving enzyme functions. *Applied Biochemistry and Biotechnology*, *143*, 212–223.
14. Bershtein, S., & Tawfik, D. S. (2008). Advances in laboratory evolution of enzymes. *Current Opinion in Chemical Biology*, *12*, 151–158.
15. Packer, M. S., & Liu, D. R. (2015). Methods for the directed evolution of proteins. *Nature Reviews Genetics*, *16*, 379–394.
16. Lutz, S., & Patrick, W. M. (2004). Novel methods for directed evolution of enzymes: quality, not quantity. *Current Opinion in Biotechnology*, *15*, 291–297.
17. Hibbert, E. G., & Dalby, P. A. (2005). Directed evolution strategies for improved enzymatic performance. *Microbial Cell Factories*, *4*, 29.
18. Johannes, T. W., & Zhao, H. (2006). Directed evolution of enzymes and biosynthetic pathways. *Current Opinion in Microbiology*, *9*, 261–267.
19. Olsen, M., Iverson, B., & Georgiou, G. (2000). High-throughput screening of enzyme libraries. *Current Opinion in Biotechnology*, *11*, 331–337.
20. Turner, N. J. (2003). Directed evolution of enzymes for applied biocatalysis. *Trends in Biotechnology*, *21*, 474–478.
21. Sunden, F., Peck, A., Salzman, J., Ressler, S., & Herschlag, D. (2015). Extensive site-directed mutagenesis reveals interconnected functional units in the alkaline phosphatase active site. *eLife*, *4*, e06181. doi:10.7554/eLife.06181.
22. Reetz, M. T. (2013). The importance of additive and non-additive mutational effects in protein engineering. *Angewandte Chemie (International Ed. in English)*, *52*, 2658–2666.
23. Acevedo-Rocha, C. G., Hoebenreich, S., & Reetz, M. T. (2014). Iterative saturation mutagenesis, a powerful approach to engineer proteins by systematically simulating Darwinian evolution. *Methods in Molecular Biology*, *1179*, 103–128.
24. Yuan, M., Yang, X., Li, Y., Liu, H., Pu, J., Zhan, C.-G., & Liao, F. (2016). Facile alkaline lysis of *Escherichia coli* cells in high-throughput mode for screening enzyme mutants: arylsulfatase as an example. *Applied Biochemistry and Biotechnology*, *179*, 545–557.
25. Feng, J., Wang, L., Liu, H., Yang, X., Liu, L., Xie, Y., Liu, M., Zhao, Y., Li, X., Wang, D., Zhan, C.-G., & Liao, F. (2015). Crystal structure of *Bacillus fastidiosus* uricase reveals an unexpected folding of the C-terminus residues crucial for thermostability under physiological conditions. *Applied Microbiology and Biotechnology*, *99*, 7973–7986.
26. Feng, J., Liu, H., Yang, X., Gao, A., Liao, J., Feng, L., Pu, J., Xie, Y., Long, G., Li, Y., & Liao, F. (2013). Comparison of activity indexes for recognizing enzyme mutants of higher activity with uricase as model. *Chemistry Central Journal*, *7*, 69.
27. Huang, S. H., & Wu, T. K. (2004). Modified colorimetric assay for uricase activity and a screen for mutant *Bacillus subtilis* uricase genes following StEP mutagenesis. *European Journal of Biochemistry*, *271*, 517–523.
28. Liu, M., Feng, J., Liu, H., Yang, X., Feng, L., Li, Y., & Liao, F. (2013). Xylenol-orange-assay-of-hydrogen-peroxide for measuring uricase activity and recognizing high-activity uricase mutant. *Chinese Journal of Applied and Environmental Biology*, *19*, 523–527.

29. Liao, F., Yang, D., Tang, J., Yang, X., Liu, B., Zhao, Y., Zhao, L., Liao, H., & Yu, M. (2009). The measurement of serum cholinesterase activities by an integration strategy with expanded linear ranges and negligible substrate-activation. *Clinical Biochemistry*, *42*, 926–928.
30. Liao, F., Zhao, Y., Zhao, L., Tao, J., Zhu, X., & Liu, L. (2006). Evaluation of a kinetic uricase method for serum uric acid assay by predicting background absorbance of uricase reaction solution with an integrated method. *Journal of Zhejiang University Science B*, *7*, 497–502.
31. Liu, B., Zhao, Y., Zhao, L., Xie, Y., Zhu, S., Li, Z., Liu, Y., Lu, W., Yang, X., Xie, G., Zhong, H., Yu, M., Liao, H., & Liao, F. (2009). An integration strategy to estimate the initial rates of enzyme reactions with much expanded linear ranges using uricases as models. *Analytica Chimica Acta*, *631*, 22–28.
32. Zhao, Y., Zhao, L., Yang, G., Tao, J., Bu, Y., & Liao, F. (2006). Characterization of a uricase from *Bacillus fastidiosus* ATCC26904 and its application to serum uric acid assay by a patented kinetic uricase method. *Biotechnology and Applied Biochemistry*, *45*, 75–80.
33. Feng, J., Li, X., Yang, X., Zhang, C., Yuan, Y., Pu, J., Zhao, Y., Xie, Y., Yuan, H., Bu, Y., & Liao, F. (2010). A new practical system for evaluating the pharmacological properties of uricase as a potential drug for hyperuricemia. *Archives of Pharmacal Research*, *33*, 1761–1769.
34. Zhang, C., Yang, X., Feng, J., Yuan, Y., Li, X., Bu, Y., Xie, Y., Yuan, H., & Liao, F. (2010). Effects of modification of amino groups with poly(ethylene glycol) on a recombinant uricase from *Bacillus fastidiosus*. *Bioscience, Biotechnology, and Biochemistry*, *74*, 1298–1301.
35. Zhang, C., Yang, X., Gao, A., Hu, X., Pu, J., Liu, H., Feng, J., Liao, J., Li, Y., & Liao, F. (2014). Comparison of modification of a bacterial uricase with N-hydroxysuccinimide esters of succinate and carbonate of monomethoxyl poly(ethylene glycol). *Biotechnology and Applied Biochemistry*, *61*, 683–690.
36. Bradford, M. M. (1976). A rapid and sensitive method for the quantitation of microgram quantities of protein utilizing the principle of protein-dye binding. *Analytical Biochemistry*, *72*, 248–254.
37. Zhao, Y., Yang, X., Li, X., Bu, Y., Deng, P., Zhang, C., Feng, J., Xie, Y., Zhu, S., Yuan, H., Yu, M., & Liao, F. (2009). Reversible inactivation of an intracellular uricase from *Bacillus fastidiosus* via dissociation of homotetramer into homodimers in solutions of low ionic strength. *Bioscience, Biotechnology, and Biochemistry*, *73*, 2141–2144.
38. Chica, R. A., Doucet, N., & Pelletier, J. N. (2005). Semi-rational approaches to engineering enzyme activity, combining the benefits of directed evolution and rational design. *Current Opinion in Biotechnology*, *16*, 378–384.
39. Lutz, S. (2010). Beyond directed evolution—semi-rational protein engineering and design. *Current Opinion in Biotechnology*, *21*, 734–743.
40. Wu, J., Yang, X., Wang, D., Hu, X., Liao, J., Rao, J., Pu, J., Zhan, C.-G., & Liao, F. (2016). A numerical approach for kinetic analysis of the nonexponential thermoinactivation process of uricase. *The Protein Journal*, *35*, 318–329.
41. Imhoff, R. D., Power, N. P., Borrok, M. J., & Tipton, P. A. (2003). General base catalysis in the urate oxidase reaction: evidence for a novel Thr-Lys catalytic diad. *Biochemistry*, *42*, 4094–4100.
42. Suzuki, K., Sakasegawa, S., Misaki, H., & Sugiyama, M. (2004). Molecular cloning and expression of uricase gene from *Arthrobacter globiformis* in *Escherichia coli* and characterization of the gene product. *Journal of Bioscience and Bioengineering*, *98*, 153–158.
43. Chen, D., Han, J., Shi, H.-N., Liu, J., Shen, L., Huo, Z., Wang, W. L., Sun, Z. D., Li, D. F., & Liu, Y. (2014). Expression, purification and activity of *Arthrobacter globiformis* uricase. *Chinese Journal of Biologicals*, *27*, 351–355.